

2.12 Behavior of Fast Reactor Fuel During Transient and Accident Conditions

Joëlle Papin, Institute for Radiological Protection and Nuclear Safety, St Paul Lez Durance, France

© 2019 Elsevier Ltd. All rights reserved.

2.12.1	Introduction	339
2.12.2	The Study of Oxide Fuel Behavior Under Transient and Accident Conditions of Sodium Fast Reactors	340
2.12.2.1	General Objectives	340
2.12.2.2	Overview of the Main Accident Scenarios Considered	340
2.12.2.2.1	Control-rod withdrawal accident	341
2.12.2.2.2	Local blockage of a subassembly	341
2.12.2.2.3	The unprotected loss of flow accident	341
2.12.2.3	The Research Approach Relative to Fuel Accident Behavior	341
2.12.3	The Fuel Behavior Under Slow Power Transients	342
2.12.3.1	The CABRI Data Base for Slow Power Transients Study	343
2.12.3.2	Fuel Melting	343
2.12.3.2.1	Influence of fuel smear density on melting occurrence (power-to-melt)	343
2.12.3.2.2	Cavity formation and in-pin fuel motion	346
2.12.3.3	Pin Thermomechanical Behavior	347
2.12.3.3.1	Low smear density fuel	348
2.12.3.3.2	High smear density fuel	348
2.12.3.4	Postfailure Fuel Behavior	349
2.12.3.4.1	Molten fuel ejection conditions with low mass melt fraction	349
2.12.3.4.2	Consequences of molten fuel ejection at low mass melt fraction	350
2.12.3.5	Fission Gas Behavior Summary	351
2.12.4	The Fuel Behavior Under Unprotected Loss of Flow Accident	351
2.12.4.1	The Experimental Simulation for the Study of the ULOF Primary Phase	352
2.12.4.2	Fuel Pin Behavior up to Failure	352
2.12.4.2.1	Fuel temperature increase and thermal expansion	352
2.12.4.2.2	Fuel pin mechanical behavior and pin failure conditions	353
2.12.4.3	Postfailure Phenomena	354
2.12.4.4	In-Pin Fuel Motion	357
2.12.5	Fuel Behavior as Consequence of a Complete Loss of Coolant in a Subassembly	357
2.12.5.1	The Degradation of the Faulted Subassembly	358
2.12.5.2	The Mechanisms of the Hexcan Melt-Through	358
2.12.5.3	The Propagation of the Molten Materials	359
2.12.6	Conclusion	360
Acknowledgment		361
References		361

Abbreviations

BFC bottom of fissile column
CDA core-disruptive accident
CRWA control rod withdrawal accident
DBA design basis accident
DND delayed neutron detection
EFR european fast reactor
FCI fuel-coolant interaction
FCMI fuel clad mechanical interaction
LOF loss of flow

Pn nominal power
PWR pressurized water reactor
SA subassembly
SFR sodium fast reactor
TD theoretical density
TIB total instantaneous inlet blockage
TOP transient over power
ULOF unprotected loss of flow
UTOP unprotected transient over power

This is a reprint of Papin, J., 2012. Chapter 2.24 – Behavior of fast reactor fuel during transient and accident conditions. In: Konings, R.J.M. (Ed.), Comprehensive Nuclear Materials, Elsevier, pp. 609–634.

2.12.1 Introduction

Since the start of the fast reactor studies, fuel behavior under transient and accident conditions has been a major safety concern with special attention given to the possible fuel melting occurrence and subsequent events. In effect, fast reactor cores under nominal operating conditions are not in the most reactive configuration and are thus highly sensitive to any fuel compaction effect that might result from fuel motion (for instance, due to melting) with the potential risk of prompt-critical events and mechanical energy release to the vessel structure. For sodium-cooled fast reactors, such potential risk is also linked to the positive reactivity feedback (in some core regions), of the sodium void effect that can generate fast power transients in the event of loss of core cooling and coolant boiling (with associated fuel pin damage and disruption).

Among the different types of fuel possibly implemented in the fast reactors (oxide, metal, nitride, carbide), the mixed oxide fuel (U,Pu)O₂ is the most largely used one. The past experience gained from operation since the 1970s of several experimental, prototype, and commercial size reactors with sodium as coolant (for instance, RAPSODIE, PHENIX, SUPER-PHENIX in France, KNK-II in Germany, JOYO, MONJU in Japan, BN-350–600 in Russia, DFR, PFR in United Kingdom, EBR II and FFTF in the United States) has provided a comprehensive knowledge on this type of fuel. Moreover, the mixed oxide fuel is also anticipated at least for the first operating phases of the future industrial prototypes within Generation IV development, with, however, a higher burn-up target objective. Therefore, this article addresses the accident behavior of mixed oxide fuel in sodium-cooled fast reactors.

The article first recalls some general points related to the study of fast reactors fuel accident behavior: objectives, main accident scenarios considered as reference for safety assessment of sodium-cooled fast reactors and related R&D approach. Then, the main phenomena occurring in the irradiated oxide fuel pins under different accident conditions are described, focusing on the fuel pin behavior up to failure and onset of pin degradation: fuel melting, mechanical loading of the cladding and failure mechanisms, fission gas behavior and molten fuel ejection into the coolant channel. The phenomena related to the late phase of the accidents with extended degradation of the fuel pins, of the subassembly or of the whole core are not detailed but only mentioned for completeness.

2.12.2 The Study of Oxide Fuel Behavior Under Transient and Accident Conditions of Sodium Fast Reactors

2.12.2.1 General Objectives

As for all types of reactors, the evaluation of fuel behavior under transient and accident conditions is an important part of the safety studies and assessment of the sodium fast reactors.

Many transients and potential initiators of accident sequences are considered and classified within design basis accidents or in the severe accident domain, according to their frequency of occurrence and to the severity of their consequences with regard to potential radiological releases to the environment (physical protection objective).

In the case of accidents within design basis for which radiological releases below stringent limit values have to be guaranteed, a precise quantification of the fuel transient behavior is needed in order to be able to check the compliance of the key parameters with the design limits and safety criteria, and also to evaluate the margins relatively to these design limits. For instance, with regard to fuel element, slow power transients during operation with protection insured by the emergency shut-down systems, should not lead to pin failure: to follow this requirement, criteria on maximal clad temperature and on the absence of fuel melting inside the pin are settled in order to guarantee pin integrity in such operational transients (the fuel element design is defined with the objective to withstand such transients all along its life) and computational tools are used to demonstrate the fulfillment of the requirement.

In case of severe accidents (design extension conditions), the study and evaluation of the fuel behavior and associated consequences are also needed in view of:

- The establishment of appropriate measures for prevention, management of the accident, and minimization of its consequences (for instance, implementation of improved detection, mitigation, and passive systems).
- The examination of the efficiency of the implemented measures.

These considerations are the basis for the safety research and development studies that were initiated since the start of fast reactor development with oxide fuel (from around 1960).

2.12.2.2 Overview of the Main Accident Scenarios Considered

For sodium fast reactors, with regard to the risk of local or generalized core melting, three main types of transient and accident scenarios are considered as references for the study of fuel transient and accident behavior:

- The slow power transient representative of one control-rod withdrawal (local fault),
- The loss of cooling due to blockage of a subassembly (local fault), and
- The unprotected loss of flow (ULOF) accident that might lead to a core disruptive accident (CDA, generalized accident).

Through the study of these scenarios (local, global accidents) that consider extreme conditions and consequences, the phenomenology of other accident sequences, due to less severe transients or to other initiators leading to similar phenomena, is also addressed.

2.12.2.2.1 Control-rod withdrawal accident

Slow power transients due to control-rod withdrawal are the most common transients occurring during reactor operation as they are used for regulation of the core power by the operators. In case of an inadvertent control-rod withdrawal due to inadvertent operator action together with a postulated dysfunction of the various protection systems, this transient might lead to severe consequences. For instance, in the French Superphenix reactor, the unprotected control-rod withdrawal accident (CRWA) has been identified as one of the most likely initiating events for a core melt accident (probability was evaluated to 3.9×10^{-6} per year). It is characterized by a slow power increase (about 1%–3% Pn/s, Pn: nominal power) and may lead to partial fuel melting inside the pins of the subassemblies surrounding the control rod. In case of an adventitious clad failure of one of those fuel pins (for instance, due to an initial defect), molten fuel ejection, even at low melt fraction of 10%–20%, and pin-to-pin failure propagation leading to whole subassembly degradation might take place and result in core melting extension and critical events. The consequences of such an accident depend on the reactor core size, mode of control-rod operation, and respective detection capabilities: in the case of a large core, local core effects of overpower may be more pronounced than in a small core in which global overpower can be early detected by usual control systems leading to power shut down.

2.12.2.2.2 Local blockage of a subassembly

Local blockage formation in a fuel assembly due to ingress of some external material into the bundle may lead to pin failure with subassembly degradation and melting, depending on the nature and geometry of the blocked zone. As a bounding case of the different types of subassembly blockages (local, total but progressive), the hypothetical total instantaneous inlet blockage (TIB) of a subassembly at nominal power has been postulated as potential initiator for a core melt accident in the frame of EFR (European fast reactor) studies. Owing to the complete and fast loss of flow in the faulted subassembly, the usual detection systems are not operating in due time (outlet temperature increase in a subassembly, delayed neutron detection (DND)) so that core power cannot be shut down early. The accident is characterized by overheating and melting of the fuel pins, degradation of the Subassembly (SA), wall failure, and possible propagation of molten materials into neighboring subassemblies and further extension of the melting process. The main safety issue is the risk of propagation of the accident beyond the neighboring subassemblies that might lead to critical events and generalized core melting.

It should be noted that for the Fermi-1 reactor, subassembly blockage caused by a piece coming loose from the Zr core catcher in the reactor vessel led to a core melt accident on October 5, 1966. Since then, recommendation to design inlet nozzles preventing blockage formation was made (no axial flow).

2.12.2.2.3 The unprotected loss of flow accident

The ULOF accident is considered to be the result of loss of primary pump flow due to potential initiating events such as electrical break-down without reactor scram. The first phase (some seconds), leads to sodium flow reduction (kinetics depending on pump inertia characteristics) and to associated power reduction linked to reactivity feedback; thereafter (some seconds later), the power to flow ratio increases so that sodium temperature reaches sodium saturation level (boiling onset). Due to the positive 'sodium void effect' in the central core regions, the ULOF leads to sodium boiling and channel voiding and may result in a CDA with a primary core power excursion (TOP, transient over power) that initiates generalized core degradation: fuel melting, clad failure and/or melting, fuel ejection into coolant with possible thermodynamic interaction, molten materials motion, fuel dispersal and relocation into the channels, and possible mechanical energy release. Beyond the primary excursion, recompaction phenomena, formation of large molten pools with melting of the subassembly walls may occur (transition phase) and lead to a secondary power excursion (recriticality events); then an expansion phase due to fuel or sodium vapor bubble may cause significant mechanical energy release to the structures (and potential consequences on sodium spray fire after ejection into the containment vessel).

It is to be underlined that although this accident is initiated by a loss of coolant flow, it may rapidly evolve toward a fast reactivity insertion accident; therefore, it also addresses the similar phenomenology resulting from an uncontrolled passage of gas bubbles inside the core which may lead to a fast power transient (UTOP, unprotected transient over power) linked to sodium void positive reactivity feedback. In addition, it can also be noticed that the phenomena occurring beyond the primary excursion phase (transition phase, ...) have close links with the propagation of a local fault accident to neighboring subassemblies due to fuel melting.

The ULOF accident phenomenology also has close links with another loss of flow accident that is considered as potentially leading to core damage: the so-called 'LIPOSO' (DBA accident for Superphenix), caused by the break of one of the pipes between the primary pumps and the diagrid. Such an event leads to a rapid loss of flow (down to half nominal value within about 1 s) inside the core and to sodium and clad temperature increase in the outlet of the subassemblies together with a slight power increase. In case of a late detection by outlet sodium temperature increase, the main safety concerns are the risk of sodium voiding due to sodium boiling occurrence or to clad failure with potential fission gas escape, phenomena that are also addressed in the ULOF sequence.

2.12.2.3 The Research Approach Relative to Fuel Accident Behavior

Since the start of sodium fast reactor studies, the investigation of fuel accident behavior has been performed through in-pile experimental programs that used oxide fuel pins submitted to typical transient conditions as compared to reactor (neutron heating mode, thermo-fluid conditions of sodium flow, fuel and clad temperatures, slow or fast power transients) and thus allowed a close

simulation of the involved phenomena (although most of the reactors with transient test capabilities provided only tests under thermal or epithermal neutron spectrum).

In particular, during transients, the fuel accident evolution is governed by thermal and mechanical effects intimately coupled with fission gas and solid fission product behavior so that only neutron heating mode is able to provide a reliable simulation of the events.

Moreover, the initial state of the irradiated fuel before the accident, is determined by the thermomechanical and physicochemical phenomena that occurred during in-reactor normal operation and resulted in structural and mechanical changes in both fuel and cladding materials; those changes (i.e., fission gas accumulation and release, cladding swelling and embrittlement, pellet-clad gap size variation and composition, etc.), depending on temperature level and burn-up evolutions, may jeopardize the ability of the fuel pins to withstand thermal and/or mechanical loads as consequence of design basis accidents and influence the phenomena during severe accidents, and cannot be simulated without the use of realistic irradiated fuel pins.

General information on fast oxide pin designs, assembly designs, and on fast oxide fuel behavior and performance during in-reactor operation can be found else where in this volume.

Among the experimental programs, the TREAT¹ program (United States) was firstly dedicated to the study of fast power transients as consequences of ULOF and later addressed slow power ramps; the SLSF² program (United States), the German programs MOL-7B and MOL-7C in BR2 reactor,^{3,4} and the SCARABEE⁵ program (France) addressed the loss of cooling phenomena (flow blockage, loss of flow).

The most comprehensive contribution to fuel behavior studies comes from the CABRI test programs that were carried out as a common research program by the French IRSN (Institut de Radioprotection et de Sûreté Nucléaire, formerly IPSN) in conjunction with the French CEA (Commissariat à l'Energie Atomique) and the German Forschungszentrum Karlsruhe (now Karlsruher Institut für Technologie) as Senior Partners over the period 1973–2001, within a large international collaboration in part time with the United Kingdom, US/DOE, and US/NRC and with an important contribution from Japan. The first experiments (single pin geometry) were dedicated to fast UTOP and ULOF simulations using fresh fuel or low irradiated fuel pins; then, the data base was extended to industrial pins irradiated in Phenix and PFR reactors at different burn-up levels (up to 12 at%) and with various pellet geometry (solid, annular pellets), and to slow power transients. It is to be noted that the length of the fast reactor fuel columns (in the range of 0.85–1 m) being close to CABRI core height (0.8 m), allows a direct use in the CABRI⁶ facility without any need of reconditioning (unlike Pressurized Water Reactor (PWR) fuel rods). Moreover, the hodoscope device used in both TREAT and CABRI facilities and measuring fuel motion during transients (and also initial and final pin states) provides a quantified understanding of the fuel pin behavior.⁷

In relation with the experimental programs, computational tools were continuously developed in the different countries and used for analysis of the tests and evaluation of the consequences of the studied accidents of fast reactors. The fuel performance codes such as TOSURA, GERMINAL^{8,9} were developed and provide the state of the fuel after irradiation as initial fuel conditions at the beginning of an accident sequence. The accident codes PHYSURAC, PHYSURA-Grappe, SURFASS (France), PAPAS-2S (Japan), CASAS (Germany), SAS-4A, and SIMMER II (United States) were developed and used; since the 1990s, the SAS-4A code was further developed through a close collaboration between France, Germany, and Japan and the SIMMER III and IV codes (respectively two and three-dimensional modeling) were developed by Japan¹⁰ and are now largely used in the Sodium Fast Reactor (SFR) community (i.e., France, Germany¹¹).

2.12.3 The Fuel Behavior Under Slow Power Transients

In a fast neutron reactor, an inadvertent control-rod withdrawal generates a linear power increase of about 1% Pn/s in the pins located close to the control rod; this results from the reactivity insertion typically below few cents per second balanced by the negative reactivity feedback due to fuel thermal effect (Doppler effect, axial fuel expansion).

Fast reactor fuel pins operate at high linear generation rate (in the range of 40–50 kW m⁻¹, i.e., above standard values of light water reactor fuel) and with an axial power profile of cosine shape leading to a peaking factor of 1.2–1.3. In case of mixed oxide fuel with low thermal conductivity, this results in high operating temperature (around 2300K at the center and 1000K in periphery of the fuel pellet) and in possible fuel melting occurrence under transient overpower. It is to be noted that although metallic fuel is characterized by much lower steady-state operating temperature due to its higher thermal conductivity, its relative margin to melting is similar to oxide with $T(\text{nominal average})/T_{\text{melt}}$ around 80%.¹²

Moreover, in spite of high fission gas release rate observed with irradiated fuel due to high operation temperature (60%–80% fractional release at moderate to high burn-up level and mainly from the hottest center zone), power increase and subsequent high temperature also activate fission gas-related phenomena¹³ that influence thermal and mechanical pin behavior such as:

- Intragranular gas migration toward grain boundary related to thermal gradient,
- Gas bubble growth due to coalescence, vacancy diffusion (and migration for intergranular bubbles),
- Fission gas-induced fuel swelling driven by transient evolution of hydrostatic fuel pressure and bubble pressure versus temperature,
- Saturation and interconnection of grain boundary bubbles leading to additional gas release to the free volumes.

Table 1 Main characteristics of the irradiated fuel pins used in the slow power transients performed in the CABRI experimental programs (CABRI-2, FAST, RAFT)

Fuel pin	<i>Ophelie-6</i>	<i>Scarabix (Superphenix type)</i>	<i>Viggen-4 (Phenix type)</i>
Pellet geometry	Annular pellets	Annular pellets	Solid pellets
Cladding: Φ inner/outer diameter $\times 10^{-3}$ m (as fabricated values)	7.5/8.65	7.37/8.5	5.65/6.55
Fuel: Φ inner/outer diameter $\times 10^{-3}$ m (as fabricated values)	2.0/7.27	2.0/7.13	0.0/5.42
Fuel smear density (%TD, %theoretical density)	82.9	82.8	88
Maximum burn-up (at%)	4.9	6.4	11.5
Cladding material (stainless steel)	316 CW	15–15 Ti CW	15–15 Ti CW

The present understanding of irradiated fuel pins behavior under such slow power ramps mainly refers to the outcomes of the CABRI tests.^{14–17} According to the safety concerns, the objectives were to determine the power corresponding to fuel-melting occurrence ('power-to-melt'), the failure mechanisms with evaluation of the margin-to-failure (margin-to-failure is given by the difference between power level at which pin failure is expected and power level of an emergency reactor scram), and the possibility and conditions of molten fuel ejection into sodium channel in case of an adventitious clad failure with low fuel-melting fraction.

It can be underlined that under slow power transients, fuel heat generation and heat removal by the sodium coolant are almost in thermal equilibrium: these 'quasi' steady-state conditions allow the evaluation of the power level at which fuel melting occurs. These conditions then may serve for definition of the operating power limit as fuel melting onset is a first step prior to pin degradation.

2.12.3.1 The CABRI Data Base for Slow Power Transients Study

Industrial oxide fuel pins of various designs and irradiated in the Phenix reactor were submitted to slow power transients; the main characteristics of both the fuel pins and tests are respectively summarized in [Tables 1](#) and [2](#).

More details on the pins characteristics are given in Charpenel *et al.*¹⁴ and Fukano.^{15,16}

2.12.3.2 Fuel Melting

Fuel-melting occurrence depends on pin thermal behavior that is governed by thermal conductivity and heat exchange between fuel and clad through the pellet-clad gap and on melting temperature, most of these factors being function of burn-up level and of irradiation history.

In effect, melting temperature of oxide fuel depends on fuel composition (PuO_2 fraction), on burn-up level and on deviation from stoichiometry: the higher the values of these parameters, the lower the melting temperature.¹⁸

Fuel thermal conductivity depends on temperature, O/M ratio, porosity, and burn-up (see reference Carbajo¹⁸ for more information). Heat exchange through pellet-clad gap is a function of the evolution of the gap thickness and of its composition (at peak linear rating close to 40 kW m^{-1} , gap closure occurs at around 1 at% burn-up, gap composition is linked to fission gas release under irradiation and transient). At burn-up higher than 7 at%, the formation, of a bonding layer of fission products compounds inside the gap (so called 'JOG') may also influence the thermal behavior under slow power transients but uncertainty still exists on its impact.

2.12.3.2.1 Influence of fuel smear density on melting occurrence (power-to-melt)

With low smear density fuel, a significant effect of the retained fission gas on the degradation of fuel thermal performance at overpower conditions has been highlighted by the existing data base.

Such effect was derived from the striking results of the E9 and E9 bis tests indicating earlier onset of fuel melting (detected by in-pin fuel motion, thanks to the hodoscope measurement) and larger melting extension than initially predicted; for instance, in the E9 test, the power at fuel melting onset was 73 kW m^{-1} in the CABRI neutron flux, while initially predicted at 85 kW m^{-1} (it is, however, to be noted that due to the thermal spectrum of CABRI reactor causing a radial flux depression, these values need to be corrected by calculation for evaluation of the power-to-melt under a flat radial power profile as in fast neutron conditions).

In effect, due to irradiation, rare gases (Xe, Kr) are precipitated in intra- and intergranular bubbles. When fuel temperature increases during the slow power transient, and depending on the fission gas radial retention profile, the following main mechanisms take place:

- Migration of intragranular gas toward grain boundary due to diffusion and linked to thermal gradient,
- Intergranular gas bubble growth due to vacancy diffusion (relaxation of overpressure caused by temperature increase and migration from intragranular gases),
- Transient fission gas-induced swelling of the solid fuel from intergranular and porosities gases,
- Together with high-temperature plastic fuel creep into free volumes.

Table 2 Main characteristics of the slow power transient tests performed in the CABRI experimental programs

Tests	Objective	Power transient	Main results
E9 (Ophelie-6 pin)	Power-to-melt and margin-to-failure of a low smear density fuel (annular pellet)		No pin failure, large melting extension (average mass melt fraction $\sim 57\%$)
E9 bis (Ophelie-6 pin)	Cladding with reduced thickness at peak power node (to promote failure and possible ejection)		No pin failure, large melting extension (average mass melt fraction: 40%–50%)
E12 (Viggen-4 pin)	Power-to-melt and margin-to-failure of a high smear density fuel at high burn-up		Pin failure with limited fuel melting extension (average mass melt fraction around 10%)
BCF1 (Viggen-4 pin)	Influence of the power ramp rate on power-to-melt and on margin-to-failure of a high smear density fuel		Pin failure with limited fuel melting extension (average mass melt fraction $\sim 10\%$), no influence of power ramp rate on melting and failure conditions (from comparison to E12 test result)
PFX (Scarabix pin)	Power-to-melt of an annular fuel pellet (Superphenix type)		No pin failure, melting onset power level
PF1 (Scarabix pin)	Power-to-melt of an annular fuel pellet (Superphenix type)		No pin failure, average mass melt fraction $\sim 10\%$
MF2 (Scarabix pin)	Margin-to-failure of an annular fuel pellet (Superphenix type)		No pin failure, large melting extension (maximum fractional melting radius $R_m/R_0 > 80\%$)

Table 2 Continued

Tests	Objective	Power transient	Main results
RB1 (Scarabix pin with notch)	Fuel ejection in case of an adventitious pin failure with 10% average mass melt fraction		Imposed pin failure, no fuel ejection with ~10% average mass melt fraction
RB2 (Scarabix pin with notch)	Fuel ejection in case of an adventitious pin failure with 20% average mass melt fraction		Imposed pin failure, molten fuel ejection with ~20% average mass melt fraction

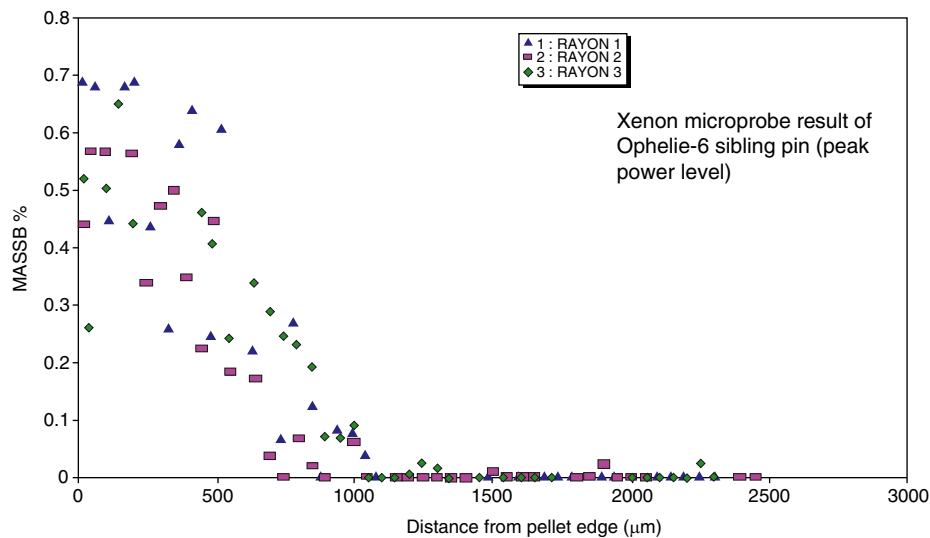


Fig. 1 Xenon radial profile from the microprobe examinations on Ophelie-6 sibling pin (axial level close to peak power location) illustrated by the Xenon mass percentage relatively to the total fuel mass of the microprobe sample (y-axis) versus distance from pellet edge (x-axis).

This may lead to central hole reduction and to increase of the macroscopic fuel porosity with subsequent reduction of the thermal conductivity and thus higher fuel temperature in the center that results in a lower power at melting onset. The consequences of this mechanism were enhanced in E9 and E9bis tests due to the low power level ($2/3 P_n$) at the end of irradiation of the Ophelie pins in the Phenix reactor that led to a high retention of fission gases (intragranular) in the equiaxed zone of the fuel pellet with potential for migration to the grain boundary (intergranular gas and porosity) and fuel swelling during thermal transient.

This significant gas retention over a 1 mm thick zone (from the pellet periphery) is illustrated by Fig. 1 showing the radial profile of the Xenon mass as given by microprobe measurements (representing the intragranular gas) at the peak power level of the Ophelie sibling pin.

As an example, the micrography of a radial cut of the E9 test pin in the Fig. 2 exhibits a decrease of fuel density and fuel fragmentation in the unmolten zone of the fuel pellet due to the slow power transient.

The impact of the fission gas-induced swelling on the fuel microstructure evolution and degradation of fuel thermal conductivity generated the need of improved physical modeling in calculation tools that provided consistent analysis of the data base.

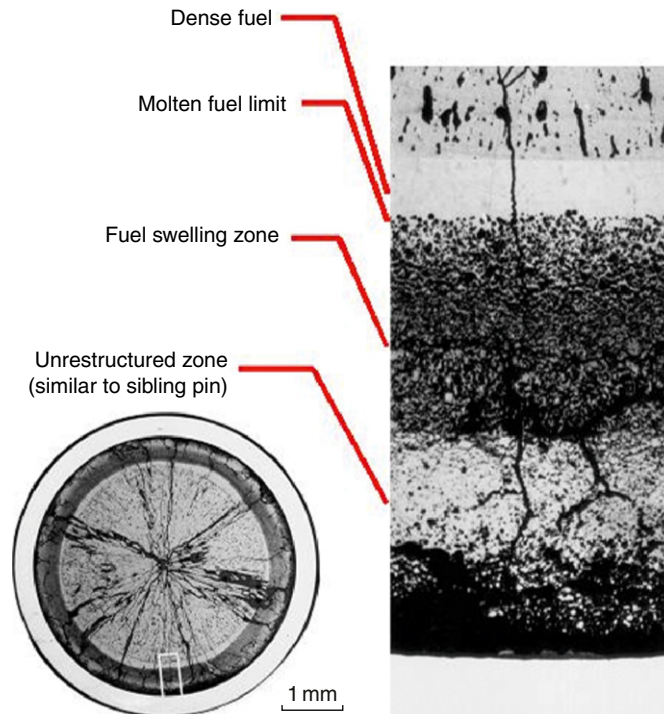


Fig. 2 Radial cut micrograph of CABRI E9 test. Reproduced from Charpenel, J., Lemoine, F., Sato, I., Struwe, D., Pfrang, W., 2000. Nucl. Technol. 130, 252–271.

In particular, simulation of this mechanism also allowed a correct determination of the power-to-melt of the Scarabix pins from the PFX experiment (78 kW m^{-1} under CABRI neutron flux). Such effect was also the basis for the limitation of the operating power of the Superphenix reactor in order to fulfill the requirement of no fuel melting during a control-rod withdrawal event.

Uncertainty still exists on fuel creep properties at high temperature (close to melting) and on high burn-up impact as almost no data is available for annular fuel type beyond 6.4 at% and submitted to slow power transient (for instance, thermal and mechanical effect of the JOG layer under slow power transient).

With high smear density fuel (solid pellet design) and even at a high burn-up of 12 at% as in the Viggen-4 pin tests, fission gas-induced swelling has a limited effect on degradation of fuel thermal behavior as compared to low smear density fuel, since less free volume is available for porosity increase and reduction of thermal conductivity. In addition, the thermal effect of JOG during transient is also lowered as the high potential for fuel-clad mechanical interaction (FCMI) of high smear density fuel leads to axial extrusion of the viscous compounds of this layer.

So, it can be stated that the fission gas retention (including radial distribution and form) due to in-reactor irradiation together with the fuel pellet smear density (or pellet design) play a major role on fuel melting occurrence during slow power transients. This stresses the high importance of the irradiated fuel state before the accident transient (so called 'T0 state'). In particular, it is underlined that with low smear density fuel, operation at low power level leading to a high quantity of retained gases in the intermediate zone of the pellet may induce low power-to-melt in case of control-rod withdrawal transient.

In the future, as low smear density fuel type is anticipated (especially with regard to mechanical aspects, see Section 2.12.3.3) together with high burn-up objectives, attention should be paid on fission gas retention and radial location with potential evolution of microstructure and on high burn-up impact on power-to-melt.

2.12.3.2.2 Cavity formation and in-pin fuel motion

Fuel melting firstly occurs in the pellet center and leads to the formation of an internal cavity filled with molten fuel and fission gases initially retained inside the fuel.

The cavity is pressurized (some tenths of MPa) by the high temperature gases and acts as a compressible volume. The gradual evolution of the cavity depends on both radial and axial fuel melting extension and also on axial fuel relocation into the available free volume as a consequence of pressure built-up within the fuel-gas mixture (foam).

According to pellet geometry, molten fuel firstly moves through the central hole (created by irradiation or by design) toward the blanket pellets in case of solid fertile pellets, or toward the plenum in case of hollow fertile pellets. This fuel motion (fuel squirting) is governed by the following parameters:

- The pressure difference between the foam and the trapped gases in the central hole or in the plena,
- The size of the central hole that influences drag forces,

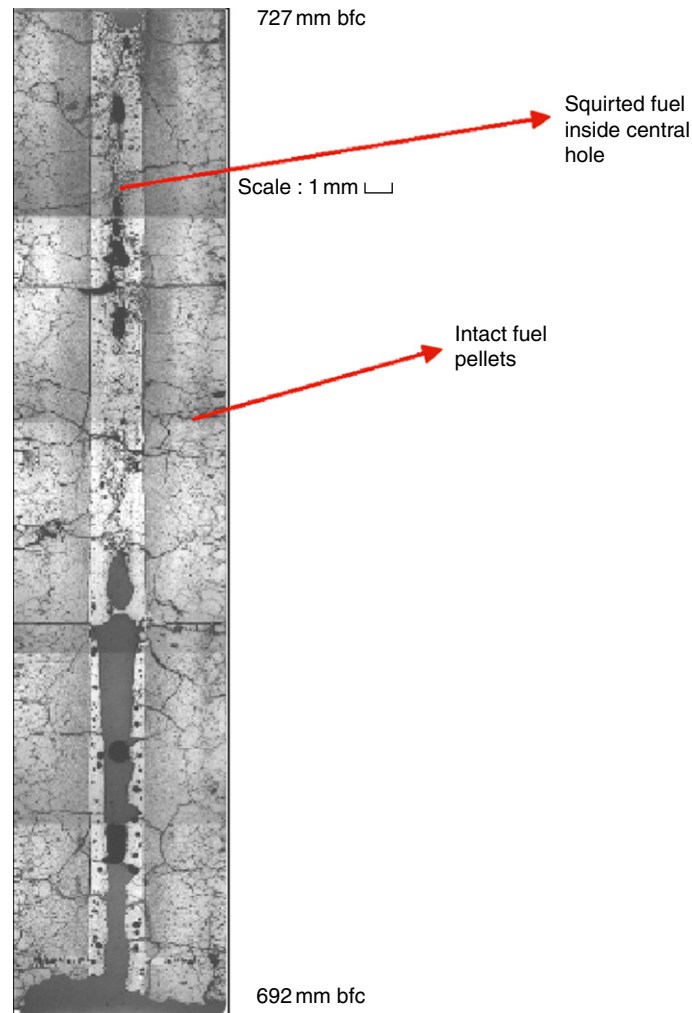


Fig. 3 Axial cut of CABRI E9 test in the upper part of the fissile column showing in-pin molten motion inside the central hole and freezing of molten fuel on the intact pellets (bfc: bottom of fissile column). Reproduced from Charpenel, J., Lemoine, F., Sato, I., Struwe, D., Pfrang, W., 2000. Nucl. Technol. 130, 252–271.

- The viscosity of the molten fuel and gas mixture, function of the fuel enthalpy,
- The freezing mechanism of the fuel when in contact with cold pellets.

Under slow power ramps, and in case of annular pellets, in-pin fuel motion has been evidenced in all the tests, even when low mass melt fraction is reached (CABRI PFX, PF1 tests). In those transients with slow melting kinetics, the in-pin motion evolution is closely related to the gradual supply of molten fuel at liquidus enthalpy that spreads over several seconds; such time scale is consistent with the observed segregation of metallic fission products (in case of fast transients, fission products are dragged with the fuel on a time scale of 100 ms).

Fig. 3 shows for the E9 test, the upward motion of the molten fuel inside the central hole of intact pellets up to the top of fissile length with central hole filling. The axial motion is limited by the solid fertile pellets. In some cases, penetration above fertile may occur through available paths (as for instance, in E9bis test with fragmented fertile pellets before test).

In-pin molten fuel motion, in providing additional volume to the molten fuel mixture, leads to reduced cavity pressurization and acts as a mitigating effect for clad mechanical loading. No significant impact on reactivity feedback (negative) is expected from this in-pin motion as long as it remains limited to fissile height of the fuel pins (and also due to the small mass involved in case of the withdrawal of a single control rod).

2.12.3.3 Pin Thermomechanical Behavior

The pin thermomechanical behavior depends on fuel and clad materials properties, temperature, and burn-up level.

The in-reactor irradiation tends to reduce the ductility of the cladding material but 15–15 Ti CW cladding material, as used in the Phenix and SuperPhenix reactors, nevertheless revealed residual ductility at a high dose rate (90 dpa) corresponding to

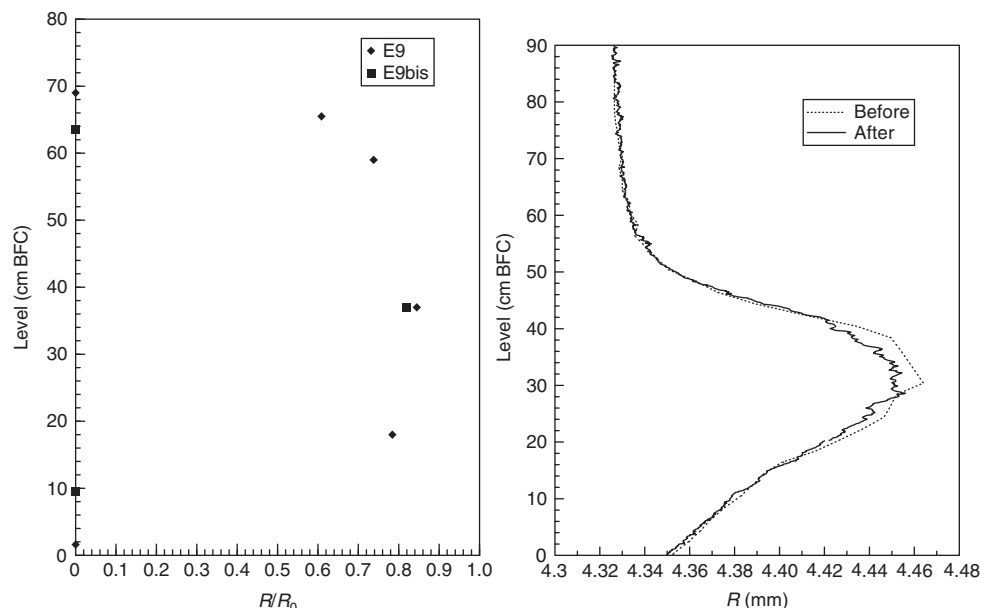


Fig. 4 Radial extension of fuel melting along fissile length in E9 and E9bis tests (right) and clad outer diameter before and after E9 test showing no deformation due to transient (left).

burn-up of 12 at% (total elongation of 4%–2% in the range of 700–800°C under low strain rate, from tensile tests on Viggen-4 cladding).

Under slow power transients, clad mechanical loading may result from fuel thermal expansion (linked to temperature increase), fission gas-induced swelling (burn-up effect) and molten cavity pressurization after fuel melting onset (if any).

2.12.3.3.1 Low smear density fuel

Within the present data base (CABRI, TREAT), low smear density fuel up to medium burn-up demonstrated high margin-to-failure and its ability to withstand high overpower conditions. Indeed, in spite of large radial extension of fuel melting (for instance, 0.86 R/R_0 in E9 test), no or very limited and local clad plastic deformation was obtained due to the transient and therefore no pin failure (only a slight deformation of 0.13% in MF2 test with 15–15 Ti CW steel was obtained). Fig. 4 shows as an example, in E9 test, the large radial extension of fuel melting along the pin and the absence of clad deformation due to transient (initial clad deformation is due to high irradiation swelling of stainless steel cold worked 316).

Such behavior is linked to the potential of low smear density fuel for mitigation of clad loading by axial in-pin motion and related limited cavity pressure built-up. Moreover, under slow power transients, no contribution of cesium (volatile fission product) on the cavity pressurization could be evidenced consistently with Cs migration in radial direction toward unmolten zone (posttest analysis of E9-E9bis tests). Therefore, it is suggested that pin failure of low smear density fuel up to intermediate burn-up, can only result from high overpower as compared to nominal value, with large melting extension and uniform pressure from cavity or from plenum, and reduced strength of the cladding due to significant clad temperature increase. In such a situation, pin failure is likely to occur in the upper part of the fissile column that is the level of maximum clad temperature under almost steady-state conditions of slow power transients (such failure mode was evidenced in some TREAT experiments¹⁶).

These points however hold for low to intermediate burn-up oxide fuel pins (up to 6.4 at%). For low smear density fuel at higher burn-up or with different fuel types, attention should be given to the potential occurrence of FCMI (Fuel-clad Mechanical Interaction) under transients, due to solid fuel pressurization and swelling before fuel melting onset. For instance, the operation period at reduced power level that leads to high fission gas inventory or the high intergranular gas retention at the periphery of the high burn-up fuel pellets, may promote FCMI loading.

2.12.3.3.2 High smear density fuel

With high smear density fuel, mechanical loading can be high enough to cause significant clad straining or even failure due to combined contribution of both mechanisms:

- FCMI from solid fuel pressurization and swelling; in particular, strong FCMI is likely with high burn-up fuel in which significant gas quantity is retained at grain boundary and porosity, in the outer zone of the pellet with fine grain structure, similarly to the rim zone of light water reactor fuel.^{19,20}
- Cavity pressurization depending on the amount of retained gas after irradiation.

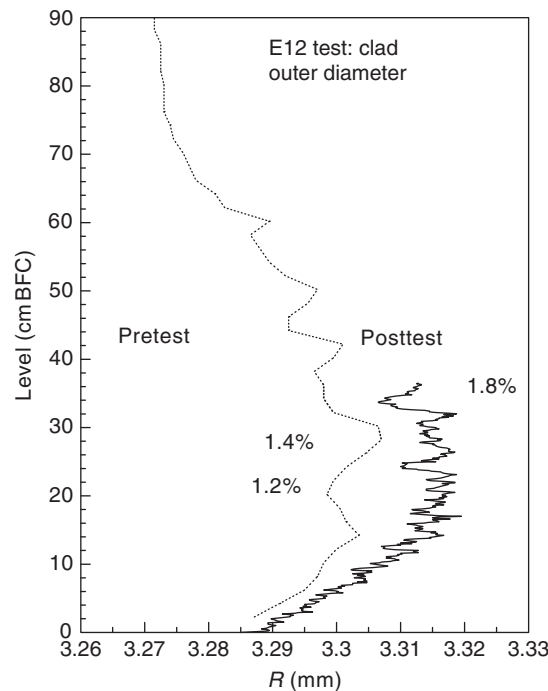


Fig. 5 Clad outer diameter before and after E12 test showing a 0.6% permanent deformation due to transient, in the lower part of the test pin. Reproduced from Charpenel, J., Lemoine, F., Sato, I., Struwe, D., Pfrang, W., 2000. Nucl. Technol. 130, 252–271.

In effect, in the CABRI E12 test pin that failed at 81 kW m^{-1} (power, however, much greater than end of life level of 31 kW m^{-1}) at the level 0.6 m from bottom of fissile length where clad temperature at failure level is in the range of 983–1013K (710–740°C) and with a limited radial extension of the molten cavity (molten mass fraction of 10%), an additional plastic deformation of 0.6% in the lower part due to transient (see Fig. 5) is obtained: this confirms that FCMI highly contributed to clad loading and failure in addition to cavity pressure.

On this basis, it can be stated that high smear density fuel has lower margin-to-failure than low smear density fuel. In addition, it is demonstrated that the pin failure threshold of high smear density fuel is not affected by the average power ramp rate in the range of 0.9%–2.8%P0/s (from E12 and BCF1 tests).

In case of high burn-up fuel, large internal clad corrosion layer (made of Cs, oxygen, steel components) with reduction of the gap might lead to an increased FCMI; however, the corrosion level is located in the upper part of the pin that is not the zone of maximum FCMI loading and no impact of this corrosion feature has been evidenced from the present slow power transient data base. Nevertheless, with future fuel designs and depending on operation conditions, attention should be paid on the risk of possible fuel-cladding chemical interaction occurrence close to the maximum mechanical loading zone.

2.12.3.4 Postfailure Fuel Behavior

2.12.3.4.1 Molten fuel ejection conditions with low mass melt fraction

The possibility and conditions of molten fuel ejection into flowing sodium is a safety concern (see Section 2.12.2.2) within the investigation of consequences of slow power transients and in case of an adventitious pin failure with low mass melt fraction.

In case of high smear density fuel and high burn-up level, evidence of molten fuel ejection at mass melt fraction of 10% (corresponding to an areal melt fraction of 20%–30% at the axial peak) is brought from failure of E12 and BCF1 test pins with the following points:

- As a result of the limited molten area, a thick shell of solid fuel is present in the outer pellet zone characterized by a high fission gas retention and high concentration of intergranular gases and pores (typical of high burn-up structure),
- Under slow transients, molten fuel is highly mobile as its enthalpy is close to liquidus value that induces low viscosity; together with high cavity pressure, this enables penetration of molten fuel through the cracks in the porous solid shell potentially inducing a release of molten fuel outside the pin and contact with sodium,
- A complete voiding of the molten cavity occurs due to its high pressure.

For low smear density fuel, pin failure with a low melt fraction is unlikely in a deterministic manner; so, the investigation of the low melt fraction leading to fuel ejection in case of an adventitious clad failure required a specific approach through the simulation

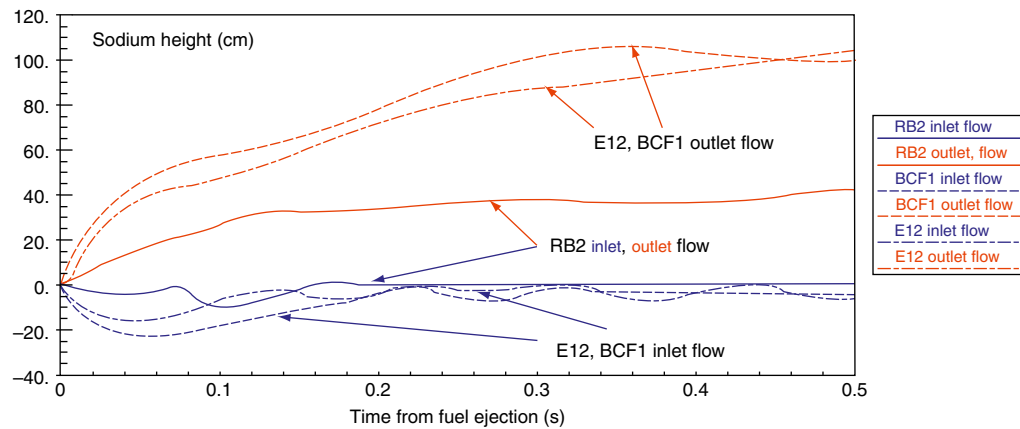


Fig. 6 Sodium channel voiding extension after clad failure in the slow transient CABRI tests E12, BCF1, RB2. (From outlet and inlet flows measurements, origin of voiding is the failure location in each test).

of an initial clad defect that is designed to fail at a given molten mass fraction. This could be performed by the use of a machined slot on the irradiated cladding of Scarabix pins, covered with a fusible material whose melting is initiated at peak power level by a small cladding temperature increase without any modification of the molten fuel fraction.

The detailed analysis of these RB1 and RB2 tests suggested that molten fuel ejection at low melt fraction is possible if the following conditions are simultaneously fulfilled:

- The melting radius reaches the limit of the solid fuel cracked zone which provides free paths for the highly mobile fuel liquid fuel,
- The cavity pressure is higher than coolant pressure (sodium pressure is about 0.2–0.4 MPa).

In terms of molten mass fraction and in case of low smear density fuel at moderate burn-up (6.4 at%), this corresponds to a threshold for molten fuel ejection to be expected between 10% and 18%. However, the validity of extrapolation of these conditions to higher burn-up fuel is not assured.

In addition, as pressure cavity is driving the fuel ejection, influence of fuel smear density is also outlined (lower fuel ejection rate with low smear density fuel as compared to solid fuel under similar low melt fraction).

2.12.3.4.2 Consequences of molten fuel ejection at low mass melt fraction

Fuel ejection into a sodium channel leads to sodium flow divergence in the first milliseconds with acceleration of sodium slugs and to voiding of the sodium channel as a result of:

- Volume displacement of liquid sodium linked to fuel ejection and liquid sodium thermal expansion to a lower extent,
- Fuel-coolant thermodynamic interaction (so called FCI) due to the contact of high-temperature fuel droplets (above 3100K) with liquid sodium (at temperature between 670 and 820K) and high heat exchanges leading to sudden vaporization of the sodium with pressure increase in the interaction zone,
- Expansion of fission gases inside the solid fuel (due to release of clad constraint) and gas release from plena through the rip site.

In case of high burn-up fuel, fission gas release from the solid outer fuel zone with high gas retention under intergranular form (as derived from E12 test) contributes to a sustained flow divergence.

Furthermore, the impact of molten fuel ejection rate, in relation with cavity pressure, on sodium-voiding extension is highlighted by the Fig. 6 showing a smaller voiding effect with annular fuel (RB2 test) than with solid fuel (E12 and BCF1 tests).

After fuel ejection, molten fuel is rapidly relocated due to freezing in the channel (no significant axial motion) and fuel accumulations are created.

Considering reactor conditions under slow power transients, such consequences of pin failure and fuel ejection at low mass melt fraction underline the potential risk of propagation of the pin degradation inside the subassembly depending on:

- The molten fuel contact with the cladding of the neighboring pins that are also partially molten and may lead to further pin-to-pin failure,
- The kinetics of blockage of the subassembly due to molten fuel freezing,
- The FCI amplitude that might enhance sodium voiding and clad melting of other pins, and generate mechanical effects linked to pressure peaks,

- The performance of detection devices for the accident (DND, noise sensors, etc ...),
- The capability of cooling down one (or several) subassembly(ies) containing the failed pin(s) taking into account the detection and power shut-down times, and the stored energy due to overpower.

2.12.3.5 Fission Gas Behavior Summary

The above paragraphs clearly underlined the major role of fission gases on fuel pin behavior under slow power transients during the whole accident sequence in relation with the fuel smear density, burn-up level and fission gas retention.

Fission gas retention and distribution (radial) govern fission gas-induced fuel swelling in solid fuel (from intergranular and porosity gas) due to temperature increase. This fission gas-induced fuel swelling is accompanied by solid fission products swelling but to clearly isolate and quantify this contribution from the one of the fission gases is difficult.

Fission gas-induced fuel swelling mainly acts on:

- Power-to-melt of low smear density fuel through evolution of fuel microstructure and degradation of thermal performance,
- Clad loading of high smear density fuel; at high burn-up level (due to outer gas rich zone with grain boundary gas) it may cause clad failure.

Fission gas retained in the molten fuel affects cavity pressure and in-pin fuel motion with impact on clad mechanical loading, and molten fuel ejection in case of pin failure.

Fission gas release inside the pin may lead to sustained voiding of the sodium after pin failure, if any (depending on the amount of available gas); it may also generate pin failure by pressure loading of the cladding at high temperature level, if no significant FCMI clad loading is at work.

For these reasons, the conditions of fuel pin irradiations are very important as they determine the amount, location (axial-radial profiles), form (intra-intergranular gas) of the retained and released gases inside the pins with potential impact on the phenomena. In particular, operating conditions at low power level (beyond some tens of days) followed by a slow power ramp up to a certain overpower level, might promote significant fission gas-induced fuel swelling and related consequences.

However, the fission gas-related transient mechanisms are complex, intimately coupled with thermal and mechanical behavior of oxide fuel at high temperature (not well known) and with irradiated cladding mechanical properties. No direct and accurate measurement of fission gas-induced mechanisms is presently possible and their kinetics is not known, so that simulation of these phenomena is not yet very precise in the available accident computer tools. For the future SFR fuels, attention should be given to these phenomena in view of knowledge and modeling improvements.

2.12.4 The Fuel Behavior Under Unprotected Loss of Flow Accident

The ULOF accident in sodium fast reactors has been worldwide studied for a long time because of its potential severe consequences such as prompt-critical events occurrence and risk of mechanical energy release to the vessel structure (cf. Section 2.12.2.2.3).

As described in Section 2.12.2.2.3, the phenomenology of the ULOF sequence can be considered along two main phases:

- The primary phase concerns the first consequences of the global loss of core cooling, starting at nominal power: sodium temperature increase, sodium boiling occurrence in the hottest part of the core and in the upper part of the fissile length due to forced convection (or at the peak power level in case of rapid flow reduction rate, below ~ 3 s halving time); then, development of the channel voiding inside the fissile zone with positive reactivity feedback causes a subsequent fast overpower transient so called 'primary excursion'; from there, fuel melting, pin failure/degradation, molten fuel ejection, FCI, fuel motion with associated reactivity feedback may occur with potential for a mechanical energy release.
- The late phase concerns the extended core degradation (transition phase) and the possible evolution toward more severe events: compaction effects with secondary power excursion, fuel dispersal, and mechanical energy release; the evolution of the accident during this phase is highly dependent on the core state at the end of the primary phase; for instance, if a significant fuel mass is definitively ejected out of the fissile zone at that time, the probability of prompt-critical events may be reduced.

However, the late phase of a ULOF accident with extended core degradation is not discussed in the following as it addresses multiphase multicomponents thermohydraulic system intimately coupled with neutron physics (which is out of scope of the article).

The present section will focus on the fuel pin behavior during the first phase of the accident (primary phase) that allows the quantification of the mechanical energy release due the transient overpower (TOP) and the evaluation of the impact of the mitigating events against reactivity insertion.

The present understanding of irradiated fuel pin behavior under fast power transients is mainly based on the outcomes from in-pile experimental programs: TREAT (up to 1987) and on the extensive data base from the several CABRI programs (up to 2001) that provided data for simulation tools development (see Section 2.12.2.3).

It is also underlined that in the reactor case, the whole accident sequence (also during the primary phase) is driven by the total reactivity coming from different contributions (positive, negative feedbacks) depending on the core design and the transient evolution. These different contributions to the reactivity versus time are important and must be taken into

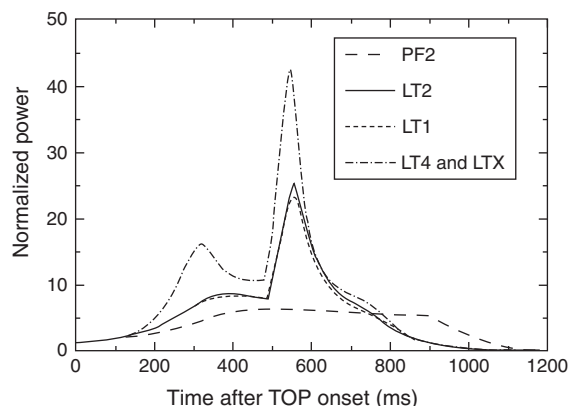


Fig. 7 Examples of medium overpower transients of the CABRI unprotected loss of flow data base.

account in the computational tools in view of reliable simulations. During the primary phase, the main reactivity contributions are:

- The sodium voiding in the central core regions generally acting as a positive feedback and dominant effect,
- The Doppler effect, the fuel axial expansion (both due to the fuel temperature increase during the transient), and the core structure dilatation (design dependent) giving a negative feedback (although not compensating the void reactivity in case of sodium boiling extension),
- The molten steel motion if any, as a positive feedback,
- The dominant impact of the fuel motion, especially due to molten fuel motion after pin failure; any axial motion toward the zone of high neutron flux results in a positive feedback, conversely, any fuel ejection out of the fissile zone has a negative feedback.

2.12.4.1 The Experimental Simulation for the Study of the ULOF Primary Phase

In the ULOF sequence and at the time of the transient overpower onset, all the sodium channels in the core are not in the same thermohydraulic state: largely voided due to boiling extension in the center, partially voided or still filled with liquid sodium in the other regions, as function of the size and design of the core. So the fuel pins in the different channels undergo the power pulse impact at different clad temperature levels and thus with different mechanical resistance and failure conditions (if any).

In the in-pile experiments, for instance, in the CABRI programs,⁶ these conditions are simulated by using single or several irradiated fuel pins cooled by a sodium flow under initial nominal power and by applying a loss of flow reduction followed by a power pulse triggered at different times corresponding to various thermal conditions of the cladding. The other main parameters investigated through the CABRI data base are:

- Various designs of the irradiated fuel pins (solid, annular pellets, different smear densities) including industrial fuel pins (from Phenix and Superphenix designs),
- Burn-up levels (different values in the range 0–12.7 at%),
- Energy injection of the TOP (range of $0.8\text{--}2 \times 10^6 \text{ J kg}^{-1}$) and energy injection rates (fast: $10\text{--}20 \times 10^6 \text{ J kg}^{-1} \text{ s}^{-1}$, medium: $1\text{--}5 \times 10^6 \text{ J kg}^{-1} \text{ s}^{-1}$) as illustrated in Fig. 7.

Detailed information on the ULOF data base and on the understanding can be found in Cranga,²¹ Fukano,²² Haessler,²³ Sato,^{24,25} Struwe,²⁶ and Wright.¹

2.12.4.2 Fuel Pin Behavior up to Failure

As a result of power transients, some phenomena that are already described in Section 2.12.3 for slow power transients also occur during ULOF sequence, however, with a different time constant. In the following, the main specific impacts of loss of flow combined with fast transients are underlined.

2.12.4.2.1 Fuel temperature increase and thermal expansion

In the ULOF accident, the fuel temperature evolution is mainly governed by the time of TOP occurrence and related energy injection (depending on the core neutron characteristics).

The first consequence is fuel thermal expansion. In the radial direction, thermal fuel expansion causes the gap closure (if it was not already closed due to high burn-up) and increase of pellet-clad heat exchange as a function of contact pressure. At high burn-up, no thermal impact of the presence of the JOG could be evidenced from the data base in those conditions. The axial

thermal fuel expansion was found to be significant, even when restrained by clad constraint (due to closed pellet-clad gap) probably because of the JOG presence (the JOG layer is in fact squeezed toward pin ends due to high contact pressure). Fuel axial expansion may amount to about $2\text{--}3 \times 10^{-2}$ m during TOP, depending on the injected energy. This effect, in reducing the fuel mass inside the fissile zone, produces a negative reactivity feedback, that is however not sufficient to stop the energy injection.

In case of a delayed TOP after onset of sodium boiling, a first significant fuel temperature increase may take place after clad dry-out (due to drastic reduction of heat exchanges from the clad to sodium) and is then followed by the TOP effect. During the LOF phase, the axial fuel expansion is limited (of the order of 4×10^{-3} m).

Under ULOF/TOP conditions, fuel melting is reached as a result of the significant fuel temperature increase. It is to be noted that in such fast power transients, the impact of fuel smear density on fuel thermal performance is not significant (on the contrary to the slow power transient behavior) because significant fuel swelling has no time to take place. A molten cavity is formed from the center of the pellets (highest fuel temperature location); under the high and fast energy injection and when clad temperature is lower than 1200K, the cavity pressure from the mixture of molten fuel and fission gases (see Section 2.12.3.2.2) is higher than in slow power ramps as a result of high cladding strength (related to high strain rate) and of fast extension of the melting zone.

2.12.4.2.2 Fuel pin mechanical behavior and pin failure conditions

The basic mechanisms driving the pin mechanical behavior are similar to those already described in Section 2.12.3.3 for slow power transients; however, in the ULOF/TOP sequence, their importance highly depends on the energy injection rate and on the clad temperature level at the time of maximum loading. Moreover, pin failure conditions have a significant impact on the follow-on of the accident as they determine the potential for molten fuel relocation and associated reactivity feedback.

Similarly to slow power transients, no significant impact of the presence of the JOG layer (high burn-up fuel) is evidenced on the pin mechanical behavior under fast TOP (due to axial extrusion).

The present understanding of the data base allows identifying the three dominant mechanisms responsible for pin failure or onset of pin degradation during ULOF/TOP accident, in addition to fuel thermal expansion:

- Molten cavity pressure loading is dominant under high-energy injection rate (fast energetic TOP, $10\text{--}20 \times 10^6 \text{ J kg}^{-1} \text{ s}^{-1}$) with clad temperatures below 1200K and results in burst type failure. Cavity pressurization is increasing with fission gas retention of the molten zone and with fuel smear density. Moreover, due to fast kinetics, the gaseous swelling mechanism in solid fuel is limited before melting onset and does not participate to the clad mechanical loading.
- FCMI loading with contribution of fission gas-induced swelling (from intergranular gases and porosities) is dominant when energy injection rate is moderate ($1\text{--}5 \times 10^6 \text{ J kg}^{-1} \text{ s}^{-1}$) or slow (see Section 2.12.3.3). FCMI due to fission gas swelling is enhanced with high burn-up fuel due to its significant inventory of grain boundary gases in the periphery of the pellets (rim zone) and also with high smear density fuel. This is highlighted by the CABRI-2 tests E2 and E3 using high-burn-up high smear density fuel (Viggen-4 fuel, see Section 3) that resulted in pin failure at a low enthalpy level (peak enthalpy) with a limited fuel melting extension and thus a limited cavity pressure (Fig. 8). FCMI loading due to fission gas-induced fuel swelling may also result from reactor operation at reduced power that enhances fission gas retention inside fuel. With high clad temperature (in the range of 970–1170K), larger fuel swelling is expected as a result of the reduced cladding strength; in such conditions and according to clad mechanical properties of irradiated stainless steel (as those already used: 15–15 Ti CW, for instance), FCMI failure potential may be increased due to low clad failure strain.
- In case of a delayed TOP after loss of flow, the high clad temperature ($T > 1300\text{K}$) and the reduced cladding strength allow significant fuel swelling to occur and result in fuel 'break-up' when fuel temperature is close to melting onset. It is underlined that this mechanism (clearly identified from the hodoscope measurements) is independent of the total injected energy, of fuel smear density, and of burn-up (except for fresh fuel in which very low gas quantity prevents from fuel swelling) as shown in Fig. 8. The high amplitude of fuel swelling in these conditions may also lead to loss of clad integrity before clad melting (clad melting temperature around 1660K) and to gas blow-out from the plenum, before fuel break-up.

When failure occurs due to cavity pressurization or FCMI loading and according to clad temperature axial profile, failure site is located above the peak power level, at around 2/3 of fissile length; when fuel pin break-up mode is at work, the onset of pin disruption occurs close to peak power level. These points are important with regard to reactivity feedback linked to further fuel motion. Moreover, when pins fail at a low fuel enthalpy level (FCMI loading), multiple failure sites may also exist if a significant amount of energy is injected after first failure.

As a general feature, the low smear density fuel shows a tendency to lower FCMI potential due to the available free volume for fuel swelling accommodation and to a reduced cavity pressure loading after fuel melting onset (if any). This is clearly outlined in the conditions of TOP with high cladding strength (clad temperature below 1200 K) by the two CABRI tests LT2 and E6, performed under similar conditions: high burn-up level (~ 12 at%), cladding material (15–15 Ti CW) and close pure TOP transients (no clad undercooling). No failure occurred with annular fuel pellet (LT2, 79% TD (theoretical density) fuel) while solid pellet fuel pin resulted in failure (E6, 88% TD fuel). It can be noted that in the unfailed LT2 Quasar pin with annular fuel, the design of the hollow fertile pellets, in providing a direct flow path for molten fuel from fissile zone to the upper and lower plena, also contributed to the reduction of the cavity pressure after melting.

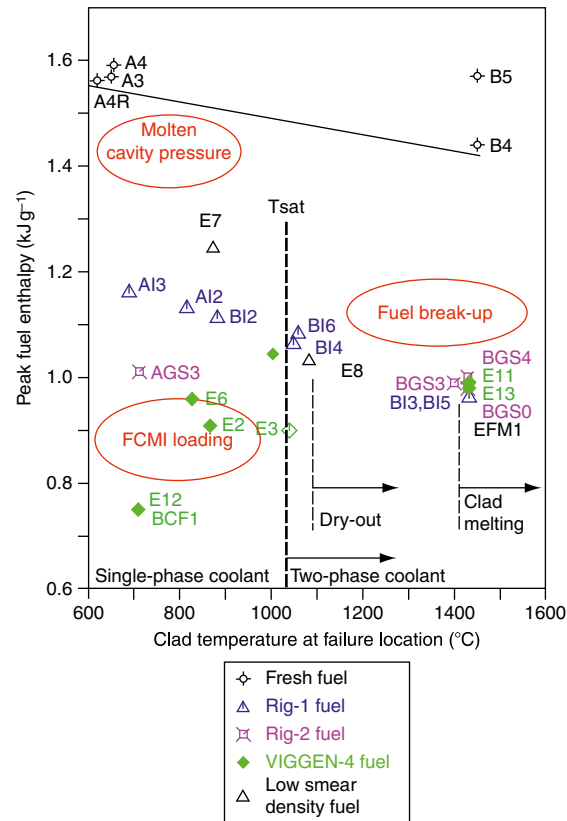


Fig. 8 Peak fuel enthalpy versus clad temperature in some CABRI tests with different fuel pins (Rig-1, Rig-2, Viggen-4 fuel, respective burn-up of 1, 2.9, and 12 at%, solid pellet; Ophelie-6 pin, 4.9 at%, low smear density fuel). Enthalpy values calculated by SAS-4A code version from D. Struwe, KIT.

Nevertheless, considering transient fission gas behavior (fuel swelling), FCMI loading may be significant even with low smear density fuel²² due to:

- Clad decreased strength caused by an undercooled overpower transient (for instance, with local undercooling),
- High fission gas-induced fuel swelling linked to high burn-up fuel occurring before fuel melting onset (before cavity formation and occurrence of fuel squirting).

In addition, in case of hollow pellet, cavity pressure is not significant before large fuel melting extension is reached and is also reduced by in-pin fuel motion. This is reflected by the high failure enthalpy threshold in the CABRI E7 test (Ophelie-6 pin, annular pellets) under fast energy injection (Fig. 8).

The Fig. 8 presents the peak fuel enthalpy (calculated value) versus clad temperature at failure location for most of the CABRI tests that led to pin failure and shows the different domains of clad-loading types and main tendencies according to the above description. The general trend of failure enthalpy decreasing with temperature is consistent with mechanical properties of irradiated cladding.

During an ULOF sequence, the loss of clad integrity due to clad melting only (with draining of molten clad) may occur in case of a delayed TOP after sodium boiling occurrence (depending on the core neutron characteristics) and if no fuel break-up is to occur (low burn-up). On the other hand, when fuel break-up occurs, intimate mixing of fuel and cladding leads to steel melting as confirmed by the transfer of metallic fission products from fuel to steel (seen on γ -scanning measurements).

These points clearly underline the impact of several parameters on the mechanical pin behavior under ULOF/TOP accident (loading and failure mechanisms) such as: irradiation history (burn-up level, fission gas retention), oxide fuel smear density, clad temperature, and transient conditions.

The modeling developed in the different simulation tools reflects the phenomena, the conditions and tendencies but uncertainty exists on failure prediction that has to be taken into account when applied to reactor calculations.

2.12.4.3 Postfailure Phenomena

The basic postfailure phenomena are similar to those described in Section 2.12.3.4 (slow TOP): fuel ejection into channel coolant, FCI, fuel pin degradation and fuel relocation. However, in comparison to slow TOP conditions, they are characterized by more energetic power transients, different channel conditions at failure (liquid sodium, partially or totally

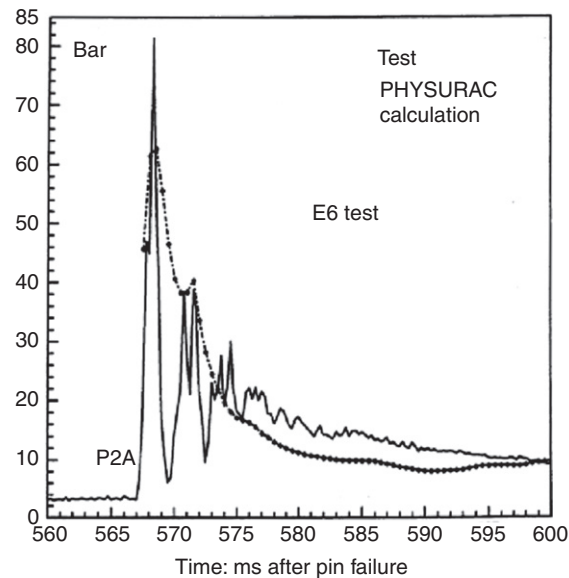


Fig. 9 Sodium channel outlet pressure as a consequence of fuel–coolant interaction after pin failure in the E6 CABRI test (experiment, PHYSURAC calculation).

voided channel), different fuel enthalpy level at failure and the fact that additional energy injection may occur after the first failure of the pin.

It is clearly outlined that the fuel ejection rate and mode depend on the fuel enthalpy level at failure time (based on the hodoscope measurements from the experimental data base). Fuel ejection rate is increased with high fuel enthalpy (from cavity pressure loading) while at low enthalpy level (due to FCMI loading), first fuel ejection is limited by pressure loss through failure rip and fuel accumulation at failure site including solid fragments from outer fuel shell. When failure occurs in a partially voided channel (high clad temperature) and at low enthalpy level, radial extrusion of solid outer fuel zone into the coolant is the dominant mode of fuel pin disruption.

In all cases, the contact of molten fuel with liquid sodium leads to FCI with related fast sodium vaporization and pressure peaks (see Fig. 9). As a result, fast channel voiding (illustrated on Fig. 10) and liquid sodium slug displacement occur with mechanical energy release.

Mechanical energy release reaches maximum values when FCI occurs in a liquid sodium channel and is lower when the channel is partially voided due to compressible zone; it increases with ejected fuel mass and enthalpy. Based on the measurements in the different CABRI test conditions, the mechanical to thermal energy ratio due to FCI is estimated to 0.7% during the first phase of sodium voiding (5 ms) and to 0.1% during the total duration of sodium expulsion: this value tends to indicate a low probability of a significant mechanical energy release due to FCI as a result of fuel ejection into sodium channel after pin failure. However, this result holds for oxide fuel. In the event of use of different fuel type in future SFR, consequences of FCI have to be checked with regard to energetic potential (for instance with carbide fuel).

In case of highly irradiated fuel, and independently of thermal–hydraulic conditions of the sodium channel at failure time, a significant amount of fission gas can be released from plena and from external parts of the fuel pellets and contribute to a sustained voiding after failure with, however, no major impact on molten fuel entrainment.

The major outcomes from the research studies devoted to ULOF/TOP concern fuel motion and relocation after pin failure. Indeed, it is clearly underlined that axial fuel dispersal and axial relocation occurring after failure is limited. The main mechanisms governing the fuel dispersal are the following:

- The freezing of the molten fuel above and below the fissile length due to bulk freezing on the leading edge (evidenced from dedicated tests²⁷) and intimate steel and fuel mixing in case of failure at high fuel enthalpy; this results in the formation of upper and lower fuel accumulations;
- In case of failure at low enthalpy level, the high viscosity of the oxide fuel under melting (fuel enthalpy between solidus and liquidus state) prevents an extended motion and the accumulation of solid fuel fragments ('chunk jamming') limits the further penetration of the foamy fuel (gas and fuel mixture).

Fig. 11 illustrates the final state of the relocated fuel in several CABRI tests simulating ULOF/TOP sequences with highly irradiated fuel pins (Viggen-4 pins, 12 at%) and shows the limited extension of relocated fuel out of the fissile zone in relation with the enthalpy level at failure or clad temperature at failure level (increasing from E6 to E11 test).

The total ejected fuel mass due to primary excursion remains lower than 20%–30% of the initial fuel mass in all cases (a higher value could be obtained in case of a delayed TOP after LOF with degradation of short upper fertile zone due to molten fuel

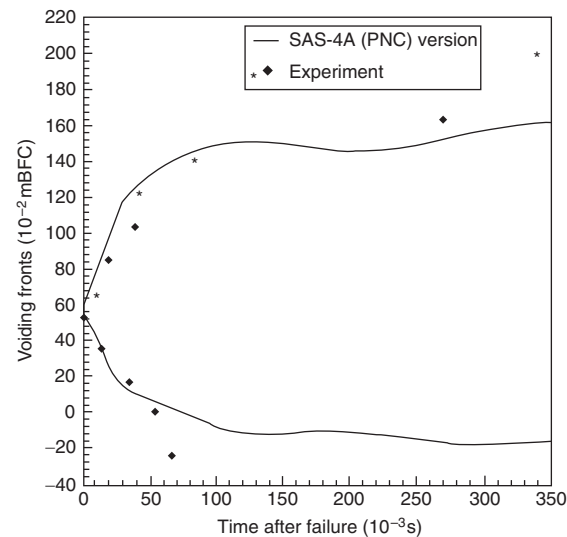


Fig. 10 Sodium channel voiding as a consequence of fuel-coolant interaction in the E6 CABRI test (experiment, SAS-4A calculation).

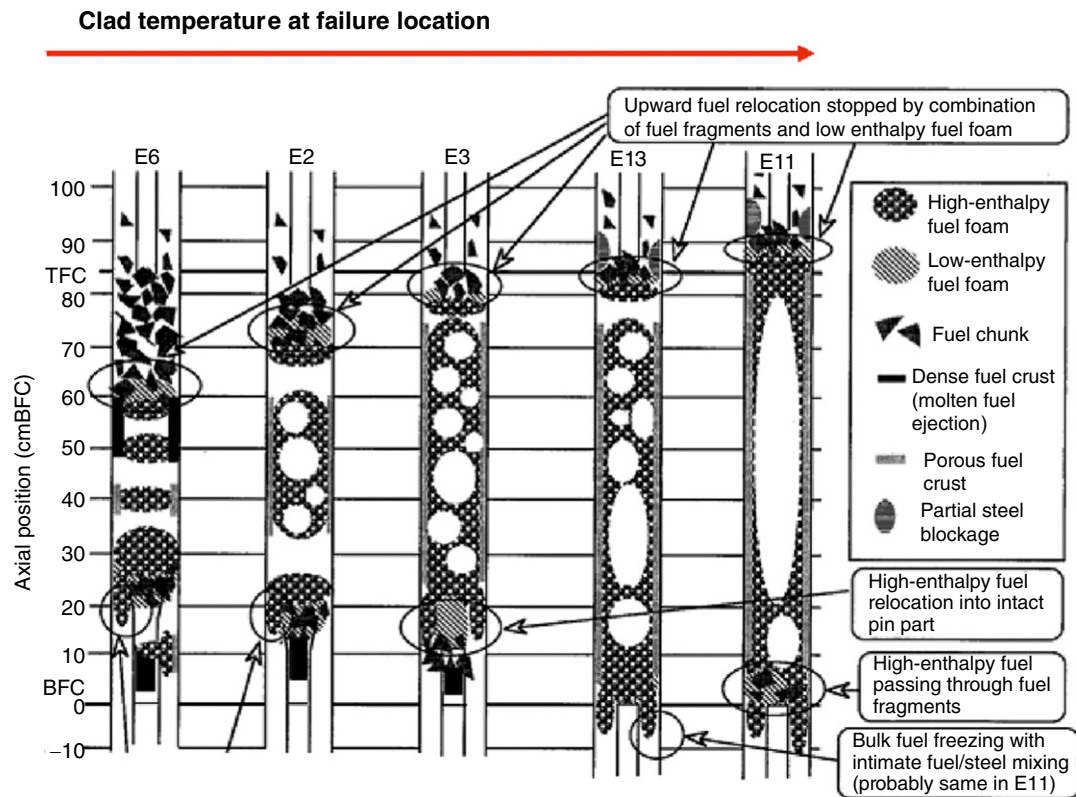


Fig. 11 Fuel relocation state at the final state of CABRI tests with high burn-up fuel (Viggen-4 pins) (white zone = materials voided zone).

contact). These findings are consistent with the results obtained in bundle geometry (TREAT results, CABRI tests performed in 3 pins bundle).

When applied to reactor calculations, the present understanding and results underline that fuel dispersal at the end of the primary excursion in a ULOF accident (in spite of negative reactivity feedback) is not sufficient to prevent the occurrence of any further critical event and that the evolution of the accident toward transition phase cannot be avoided.

In addition to prevention of ULOF accidents, reduction of the risk of occurrence of critical events during the ULOF accident sequence should be the main goal for future SFR design studies.

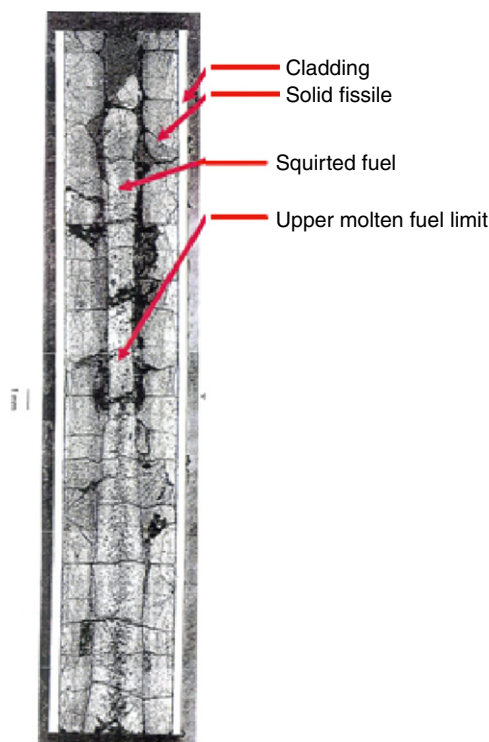


Fig. 12 In-pin molten fuel motion in the central hole of annular pellets, due to fast transient overpower (upper part of the fuel pin in CABRI PF2 test, annular pellet). PF2 axial cut: 700–735 mm from bottom of fissile length.

2.12.4.4 In-Pin Fuel Motion

In-pin fuel motion is considered during ULOF due to its potential consequences on reactivity feedback.

With annular pellets, in-pin motion of molten fuel is governed by the same mechanisms as described in Section 2.12.3.2.2 for slow power transients. So, its occurrence mainly depends on injected energy (molten fuel enthalpy and viscosity) and on clad strength (temperature $< 1200\text{K}$). The amplitude of the in-pin fuel motion is mainly limited by the freezing mechanism (bulk freezing at the front); due to fuel freezing when in contact with colder zones, fertile pellets with a central hole do not allow significant additional in-pin motion. Velocity of the in-pin molten fuel motion (derived from tests) has been evaluated to be of the order $6\text{--}9\text{ ms}^{-1}$ (faster than in slow power transients) and leads to penetration above and below the fuel melting front as shown in Fig. 12.

Under fast power transients and when the clad temperature is higher than 1200K , occurrence of in-pin motion of molten fuel is limited as pin failure occurs before any significant motion of molten fuel (especially if FCMI loading results in failure). When the overpower transient occurs in reactor conditions, the majority of the subassemblies sodium channels are partially or totally voided so that pin failures mostly occur with high clad temperature; the in-pin motion of molten fuel is thus limited and the expected mitigating effect of annular pellet design against reactivity insertion is low and has to be evaluated as a function of pins and core designs.

Another type of in-pin motion has also been evidenced from the data base: the displacement of some intact pellets from the upper and lower parts of the fissile length toward the center with potential for reactivity insertion in addition to the TOP due to sodium voiding. This phenomenon occurs with solid fuel pellet, at the end of the power transient (after pin failure). Such a motion is driven by the pressure difference between the plena and the disrupted zone and is made possible by the release of the clad constraint on the lower and upper pellets linked to the clad temperature increase at these levels. This stub motion is increased with high burn-up fuel but is, however, limited in amplitude (some centimeters) and velocity ($< 1\text{ ms}^{-1}$) and should not lead to significant increase of reactivity in reactor conditions.

2.12.5 Fuel Behavior as Consequence of a Complete Loss of Coolant in a Subassembly

The hypothetical TIB of a subassembly at nominal power is considered as a bounding case of other subassembly blockage accidents in some reactors studies (see Section 2.12.2.2.2).

The complete and fast loss of coolant prevents the early accident detection by the usual systems (measurement of the sodium temperature at the outlet of the subassembly, DND). As a consequence, there is no power shut down at the early stage of the accident sequence and the fuel pins are rapidly degraded by overheating with propagation of molten material to the surrounding

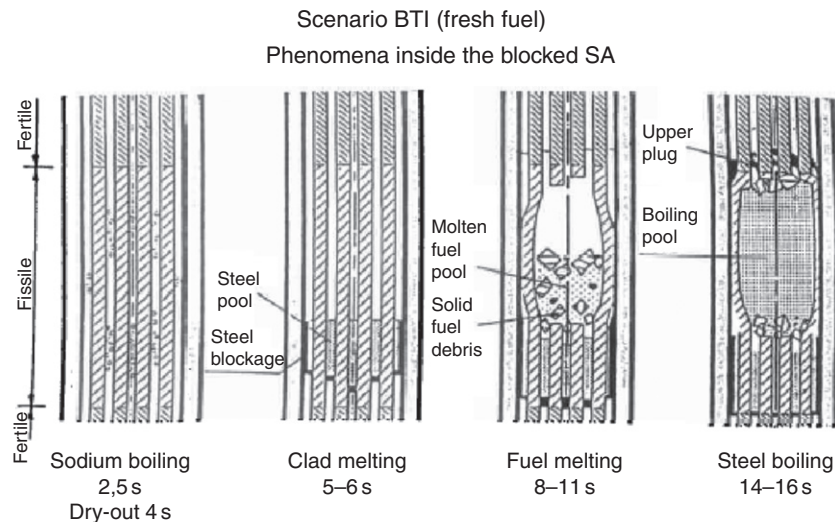


Fig. 13 Scenario of the subassembly degradation under total instantaneous inlet blockage accident with fresh fuel, as deduced from posttest examinations of the SCARABEE test series. Reproduced from Kayser, G., Charpenel, J., Jamond, C., 1998. Nucl. Sci. Eng. 128, 144–185.

subassemblies. The main safety concern of TIB is the risk of evolution of the accident toward local critical events and subsequently toward a generalized core melting.

The present knowledge related to this accident sequence, refers to the subassembly blockage studies and to the in-pile SCARABEE experimental program.^{3–5,28–33} In the SCARABEE experiments, the TIB accident was simulated by the rapid closure of an inlet sodium valve in a bundle geometry (19, 37 pins) with fresh fuel pins (fissile length of 0.6 m) at nominal power (average pin power of $35 \times 10^3 \text{ W m}^{-1}$).

2.12.5.1 The Degradation of the Faulted Subassembly

As a consequence of the undercooling of the subassembly, the fuel pin transient evolution is mainly governed by thermal effects with the following rapid scenario as illustrated on Fig. 13:

- Sodium boiling, clad dry-out, and clad melting at the level of maximum power, in the center of fissile length (absence of forced convection, cosine power profile);
- Draining of the molten cladding (sodium vapor velocity is not sufficient for upwards entrainment), formation of a tight steel blockage in the lower cold part and accumulation of liquid steel around intact fuel pellets;
- Fuel melting occurrence and mixing with molten steel leading to a local boiling pool that expands over the fissile length with formation of an upper steel blockage.

This degradation phase lasts over 14–16 s assuming nominal power conditions.

It is underlined that as in the ULOF sequence, no significant fuel mass is ejected out of the fissile length, even if small FCIs contribute to the fuel relocation in the upper part. This results in a confined pool with power generation and thus implies high thermal fluxes (value of the order of $15\text{--}20 \times 10^6 \text{ W m}^{-2}$ in a reactor case) toward the external wall (hexagonal stainless steel structure named “hexcan”). These fluxes are maintained at a high level even after power shut down, with subsequent risk of hexcan melt-through. No significant pressurization of the boiling pool due to steel vapor could be evidenced (under pressure of the order of 0.1 MPa, the steel vapor temperature is closed to fuel melting temperature).

Under the TIB conditions, the impact of irradiation is not well known and the above scenario of degradation might differ with irradiated fuel pins on the following points: improved detection capability (by DND) from the faulted subassembly (i.e., before the propagation of the accident to the surrounding subassemblies), molten pool formation with early mixing of fuel and steel owing to the fuel break-up mode (see Section 2.12.4.2.2), axial fuel ejection due to high fission gas blow-out after clad melting, high pressurization of the molten materials pool with influence on the propagation phenomena.

The degradation phase and pool formation may also differ in case of use of different oxide fuel element with axial zones of different power levels (as, for instance, with axial heterogeneous fuel column).

1.12.5.2 The Mechanisms of the Hexcan Melt-Through

After the degradation of the fuel pins in the faulted subassembly, the contact of liquid fuel with the hexcan wall (externally cooled by sodium under natural convection in the intersubassembly gap) generates a fuel crust that acts as a thermal insulating layer

between the pool and the hexcan wall (due to low thermal conductivity of the oxide fuel). Inside the molten or boiling pool, the thermal exchanges are governed by natural convection and the presence of steel inside the pool is a major point for the efficiency of the radial heat transfer.

Several mechanisms for the hexcan melt-through were evidenced from the data base:

- Thermal erosion of the cooled wall due to steel melting just under the fuel crust; molten steel is then drained away (below or through the cracks of the crust), fuel crust is broken and allows a new contact of liquid fuel with the wall of reduced thickness; this process leads to a rapid erosion of the wall unless an efficient cooling is provided;
- Flux disequilibrium between the high heat flux from molten pool and the heat removal from the external cooling of the hexcan;
- Mechanical deformation of the hexcan walls due to high temperature and/or to FCI pressure loading, that may lead to a loss of cooling (by the intersubassembly gap);
- Jet or projections of molten materials on the wall, as a result of pressure event, may initiate local erosion of the wall.

Whatever the mechanism involved, when a boiling pool exists in reactor conditions, heat fluxes toward the wall are so high that the hexcan melt-through of both the blocked and neighboring subassemblies will rapidly occur (time delay of 1 s to some seconds).

For future SFRs with new materials anticipated for the subassembly walls, the global mechanical behavior of the hexcan at high temperature level (above 1400K) with related loss of mechanical strength has to be further considered due to the potential consequences on the global scenario (creep mechanism and risk of compaction effect).

2.12.5.3 The Propagation of the Molten Materials

The hexcan melt-through initiates the propagation of the molten material⁵ in the intersubassembly gap or in the neighboring subassemblies.

The propagation of molten materials inside the subassembly gap is very limited by the formation of a resistant steel blockage (from the steel wall) that prevents further penetration of the materials (evidenced from the Scarabee PI-A test, Fig. 14).

The melt propagation in the neighboring subassembly (cooled by nominal sodium flow, Scarabee PV-A test, Fig. 15), occurs step by step due to mild FCI events and pressure peaks. These events break the steel accumulation formed on the intact pins (clad under melting) and allow progression of the melt in a symmetrical way inside the neighboring subassemblies with rapid formation of a blockage at the inlet of these subassemblies. However, neither axial fuel ejection out of the fissile zone nor energetic events due to FCI were evidenced. It is underlined that such propagation conditions are characterized by the emission of a strong delayed neutron signal that corresponds to the first significant and reliable detection capability of the accident in case of fresh fuel.

The identified degradation and propagation mechanisms in the TIB accident with fresh oxide fuel clearly outline that the short-term scenario of the accident is globally governed by thermal effects (a simple modeling could therefore be used for translation to reactor conditions in a first step).

Moreover, as the degradation of the faulted subassembly inevitably leads to the propagation into the neighboring subassemblies, the prevention of further propagation of the accident beyond the six neighboring subassemblies relies on the detection capability (short time response is needed, some seconds, along with efficiency and reliability). For future SFR, attention should be focused on the impact of irradiated fuel on the scenario (not yet addressed), on the mechanical behavior of subassembly walls at high temperature and on the capability for an early detection of the accident.

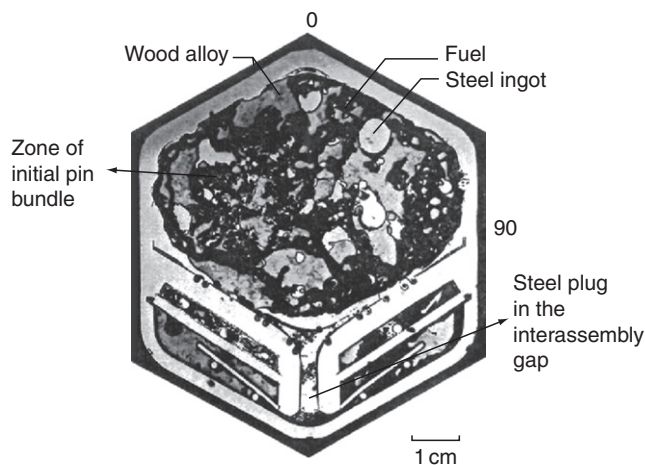


Fig. 14 Propagation in the intersubassembly as a result of a total instantaneous inlet blockage accident: experimental simulation in the SCARABEE PI-A test. Reproduced from Kayser, G., Charpenel, J., Jamond, C., 1998. Nucl. Sci. Eng. 128, 144–185.

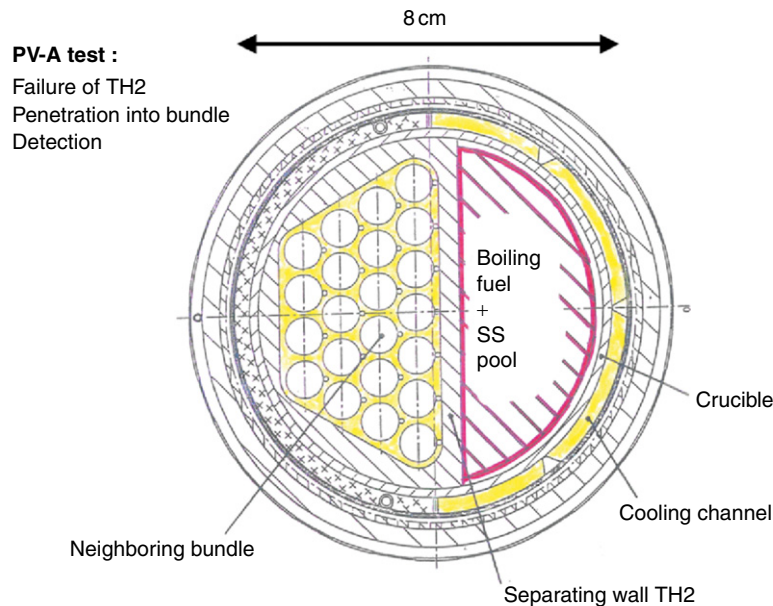


Fig. 15 Propagation of a boiling pool in a neighboring subassembly as a result of a total instantaneous inlet blockage accident: experimental simulation in the SCARABEE PV-A test. Reproduced from Kayser, G., Charpenel, J., Jamond, C., 1998. Nucl. Sci. Eng. 128, 144–185.

With regard to the risk of large propagation with potential occurrence of critical events and core melting, long-term behavior also needs to be evaluated. The related phenomenology (molten-boiling pool, propagation) is close to that of the late phase of an ULOF or to the propagation phase of an unprotected CRWA and is described by the SIMMER III tool.^{10,11}

2.12.6 Conclusion

Fuel behavior under transient and accident conditions is a major safety concern for fast reactors in relation with possible fuel melting occurrence and potential risk of prompt-critical events leading to significant mechanical energy release.

The present overview focused on oxide fuel behavior (as the most widely used for SFR up to now) and addressed typical reference scenarios that are considered within the safety assessment such as: slow power transients, ULOF and total blockage of a subassembly.

Thanks to the in-pile experimental data base, reliable knowledge on the phenomena occurring with industrial irradiated fuel pins under various representative transient conditions was provided and allowed a consistent understanding. This past experience stands as valuable guidelines to orient the innovative aspects of future SFR fuel development toward search for improved safety and reduction of recriticality potential.

The main phenomena have been identified and the influence of the key parameters on fuel accident behavior has been highlighted.

In particular, under slow power transients, low smear density fuel has evidenced a high margin for pin failure but a possible degradation of thermal performance linked to high fission gas retention that underlines the important impact of the burn-up level and of the irradiation history.

Under fast power transients in the ULOF/TOP sequence, the possible mitigating effect of annular fuel with regard to in-pin molten fuel motion and related negative reactivity feedback is not assured; the degradation mechanisms due to the primary power excursion result in a limited fuel discharge that does not prevent for further risk of critical events occurrence.

In a TIB accident, the risk of propagation of the molten materials from the faulted subassembly beyond the surrounding subassemblies highly depends on the efficiency and time response of the detection systems; impact of irradiated fuel and long-term cooling of the degraded zone should be evaluated.

Modeling of fuel transient behavior has been developed for these various transient conditions and provides a reasonable description of the accident scenarios. Such modeling concerns a wide range of phenomena that are intimately coupled together or dealing with degraded geometry: fuel and clad thermomechanical and fission gas transient behavior, failure mechanisms, postfailure events, FCI, molten pools formation and evolution, etc. However, the present modeling suffers from uncertainties that limit predictive capability to other conditions (higher burn-up, other fuel types, etc.). More accurate modeling will be needed in the future, in order to insure that design limits are not overpassed in case of design basis accidents.

Moreover, it is underlined that for future SFR, objectives of improved safety together with performance goals will induce design strategies to limit accident consequences (prevention, mitigation systems) and implementation of high-performance materials and new fuel types. Therefore, such evolution will call for additional knowledge and data base in view of development and validation of the computational tools that are needed for a robust safety approach and assessment.

Acknowledgment

The author is very thankful to Y. Guérin and M. Pelletier from CEA for their thorough review of the manuscript and valuable comments. Deep acknowledgments are also expressed to D. Struwe from KIT (Germany) and to I. Sato from JAEA (Japan), for their detailed review and comments, as long-standing partners of common safety research programs on SFR. Many thanks are also expressed to V. Georgenthum and G. Brillant from IRSN, for their critical review of the manuscript. See also chapter 2.21 Fuel Performance of Fast Spectrum Oxide Fuel.

See also: 2.03 Fuel Performance of Fast Spectrum Oxide Fuel. 2.06 Thermal Properties of Irradiated UO_2 and MOX. 2.08 Matter Transport in Fast Reactor Fuels

References

1. Wright, A.E., Dutt, D.S., Harrison, L.J., 1990. Proceedings of the International Fast Reactor Safety Meeting, Snowbird, UT, August 12–16, 1990, vol. II, p. 233. La Grange Park, IL: American Nuclear Society.
2. Thompson, D.H., Ragland, W.A., Holland, J.W., *et al.*, 1985. SLSF local fault safety experiment P4-summary and conclusions. In: Proceedings of the International Topical Meeting on Fast Reactor Safety, Knoxville, TN, p. 129. La Grange Park, IL: American Nuclear Society.
3. Peppler, W., Will, H., 1988. Nucl. Eng. Des. 110, 73.
4. Schleisiek, K., *et al.*, 1998. Nucl. Sci. Eng. 128, 93–143.
5. Kayser, G., Charpenel, J., Jamond, C., 1998. Nucl. Sci. Eng. 128, 144–185.
6. Marquie, C., Nervi, J.C., Gonner, C., Serre, F., Döderlein, C., 1999. SURA: A test facility to investigate the safety of LMFBR and PWR fuels. In: Proceedings of the International Symposium on Research Reactor Utilisation, Lisbon, Portugal.
7. Baumung, T., Lumpkin, A.H., 1986. Fuel motion measurement with the CABRI hodoscope. In: Proceedings of the International Conference on Science and Technology of Fast Reactor Safety, May 12–16, 1986, vol. I, p. 141. Guernsey, UK.
8. Melis, J.C., Piron, J.P., Roche, L., 1993. J. Nucl. Mater. 204, 188–193.
9. Roche, L., Pelletier, M., 1999. Modeling of the thermomechanical and physical processes in FR fuel pins using the Germinal code. In: Proceedings of the International Symposium on MOX Fuel Cycle Technologies for Medium and Long-Term Deployment (IAEA-SM-358/25), May 17–21, 1999. Vienna, Austria.
10. Yamano, H., Tobita, Y., Fujita, S., Mashek, W., 2009. Ann. Nucl. Energy 36, 337–343.
11. Mashek, W., Rineiski, A., Flad, M., *et al.*, 2008. The SIMMER safety code system and its validation efforts for fast reactor application. In: Proceedings of the PHYSOR, September 14–19, 2008. Interlaken, Switzerland.
12. Wigeland, R., Cahalan, J., 2009. Fast reactor fuel type and reactor safety performance. In: Proceedings of Global, September 6–11, 2009. Paris, France.
13. Olander, D.R., 1976. Fundamental Aspects of Nuclear Reactor Fuel Elements. Technical Information Center, Office of Public Affairs, Energy Research and Development Administration. (TID-26711-P1).
14. Charpenel, J., Lemoine, F., Sato, I., Struwe, D., Pfrang, W., 2000. Nucl. Technol. 130, 252–271.
15. Fukano, Y., Charpenel, J., 2004. The adventitious pin failure study under a slow power ramp. In: Proceedings of the 12th International Conference on Nuclear Engineering, April 25–29, 2004. Virginia: CD-Rom.
16. Fukano, Y., Onoda, Y., Sato, I., Charpenel, J., 2009. Fuel pin behaviour under slow ramp-type transient-overpower conditions in the CABRI-FAST experiments. In: Proceedings of the 13th International Topical Meeting on Nuclear Reactor Thermal-Hydraulics (NURETH-13), September 27–October 2, 2009. Kanazawa City, Ishikawa Prefecture, Japan.
17. Papin, J., Lemoine, F., Sato, I., Struwe, D., Pfrang, W., 1994. Fuel pin behaviour under conditions of control rod withdrawal accident in CABRI-2 experiments. In: Proceedings of the International Topical Meeting on Sodium Cooled Fast Reactor Safety, October 3–7, 1994, vol. 2, p. 134. Obninsk, Russia.
18. Carbajo, J.J., Yoder, G.L., Popov, S.G., Ivanov, V.K., 2001. J. Nucl. Mater. 299, 181–198.
19. Guérin, Y., Noiroi, J., Lespiaux, D., Chaigne, G., Blanpain, P., 2000. Microstructure evolution and in-reactor behavior of MOX fuel. In: Proceedings of the International Topical Meeting on Light Water Reactor Fuel Performance, April 16–13, 2000. Park City, UT.
20. Lemoine, F., Cazalis, B., Rigat, H., 2000. The role of fission gases on the high burn-up fuel in reactivity initiated accident conditions. In: Proceedings of the 10th International Symposium on Thermodynamics of Nuclear Materials. Halifax, Canada.
21. Cranga, M., Struwe, D., Pfrang, W., Brear, D., Nonaka, N., 1990. Proceedings of the International Fast Reactor Safety Meeting, Snowbird, UT, August 12–16, 1990, vol. I, p. 421. La Grange Park, IL: American Nuclear Society.
22. Fukano, Y., Onoda, Y., Sato, I., 2010. Nucl. Sci. Technol. 47 (4), 396–410.
23. Haessler, M., Struwe, D., Butland, A., *et al.*, 1990. In: Proceedings of the International Fast Reactor Safety Meeting, Snowbird, UT, August 12–16, 1990, vol. II, p. 209. La Grange Park: American Nuclear Society, IL.
24. Sato, I., Imke, U., Pfrang, W., Berne, M., 1994. Transient fuel pin behaviour and failure conditions in CABRI-2 in-pile tests. In: Proceedings of the International Topical Meeting on Sodium Cooled Fast Reactor Safety, October 3–7, 1994, vol. 2, p. 134. Obninsk, Russia.
25. Sato, I., Lemoine, F., Struwe, D., 2004. Nucl. Technol. 145, 115–137.
26. Struwe, D., Pfrang, W., Cameron, R., Cranga, M., Nonaka, N., 1990. Fuel pin destruction modes-experimental results and theoretical interpretation of the CABRI-1 Programme. In: Proceedings of the BNES Meeting on Fast Reactor Core and Fuel Structural Behaviour, June 4–6, 1990, p. 127. Inverness, UK.
27. Berthoud, G., Duret, B., 1989. The freezing of molten fuel: Reflexions and new results. In: Proceedings of the Fourth International Topical Meeting on Nuclear Reactor Thermal-Hydraulics (NURETH-4), October 10–13, 1989. Karlsruhe, Germany.
28. Anzieu, P., Camaro, P.Y., Lo Pinto, P., 1990. In: Proceedings of the International Fast Reactor Safety Meeting, Snowbird, UT, August 12–16, 1990, vol. IV, p. 427. La Grange Park, IL: American Nuclear Society.

29. Kayser, G., Berthoud, G., 1992. Fuel-coolant interaction in SCARABEE. In: Proceedings of the International Conference on Design and Safety of Advanced Nuclear Power Plants, October 25–29, 1992. Tokyo, Japan.
30. Livolant, M., Dadillon, J., Kayser, G., Moxon, D., 1990. Proceedings of the International Fast Reactor Safety Meeting, Snowbird, UT, August 12–16, 1990, vol. II, p. 177. La Grange Park, IL: American Nuclear Society.
31. Papin, J., Stansfield, R., 1989. Thermal-hydraulic behaviour of a fast breeder reactor subassembly during an undercooling accident: The PHYSURA-Grappe code and its validation on SCARABEE experiments. In: Proceedings of the 4th International Topical Meeting on Nuclear Reactor Thermal-Hydraulics. Karlsruhe, Germany.
32. Papin, J., Sesny, R., Soussan, P., Mac Dougall, J., Stansfield, R., 1990. The SCARABEE total blockage test series: Synthesis of the interpretation. In: Proceedings of the International Fast Reactor Safety Meeting, Snowbird, UT, August 12–16, 1990, vol. II, p. 367. La Grange Park, IL: American Nuclear Society.
33. Soussan, P., Schwarz, M., Moxon, D., Berthet, B., 1990. Propagation and freezing of molten material-interpretation of experimental results. In: Proceedings of the International Fast Reactor Safety Meeting, Snowbird, UT, August 12–16, 1990, vol. II, p. 223. La Grange Park, IL: American Nuclear Society.